Limit on the tau neutrino mass from $\tau^- \to \pi^- \pi^+ \pi^- \pi^0 \nu_\tau$

M. Athanas, P. Avery, C. D. Jones, M. Lohner, C. Prescott, A. I. Rubiera, J. Yelton, and J. Zheng

University of Florida, Gainesville, Florida 32611

G. Brandenburg, R. A. Briere, A. Ershov, Y. S. Gao, D. Y.-J. Kim, and R. Wilson

Harvard University, Cambridge, Massachusetts 02138

T. E. Browder, Y. Li, J. L. Rodriguez, and H. Yamamoto

University of Hawaii at Manoa, Honolulu, Hawaii 96822

T. Bergfeld, B. I. Eisenstein, J. Ernst, G. E. Gladding, G. D. Gollin, R. M. Hans, E. Johnson, I. Karliner, M. A. Marsh, M. Palmer, C. Plager, C. Sedlack, M. Selen, J. J. Thaler, and J. Williams

University of Illinois, Urbana-Champaign, Illinois 61801

K. W. Edwards

Carleton University, Ottawa, Ontario, Canada K1S 5B6
and the Institute of Particle Physics, Canada

R. Janicek and P. M. Patel

McGill University, Montréal, Québec, Canada H3A 2T8
and the Institute of Particle Physics, Canada

A. J. Sadoff

Ithaca College, Ithaca, New York 14850

R. Ammar, P. Baringer, A. Bean, D. Besson, D. Coppage, R. Davis, S. Kotov, I. Kravchenko, N. Kwak, X. Zhao, and L. Zhou

University of Kansas, Lawrence, Kansas 66045

S. Anderson, V. V. Frolov, Y. Kubota, S. J. Lee, R. Mahapatra, J. J. O'Neill, R. Poling, T. Riehle, and A. Smith

University of Minnesota, Minneapolis, Minnesota 55455

M. S. Alam, S. B. Athar, A. H. Mahmood, S. Timm, and F. Wappler

State University of New York at Albany, Albany, New York 12222

A. Anastassov, J. E. Duboscq, K. K. Gan, C. Gwon, T. Hart, K. Honscheid, H. Kagan, R. Kass, J. Lorenc, H. Schwarthoff, E. von Toerne, and M. M. Zoeller

Ohio State University, Columbus, Ohio 43210

S. J. Richichi, H. Severini, P. Skubic, and A. Undrus

University of Oklahoma, Norman, Oklahoma 73019

M. Bishai, S. Chen, J. Fast, J. W. Hinson, J. Lee, N. Menon, D. H. Miller, E. I. Shibata, and I. P. J. Shipsey

Purdue University, West Lafayette, Indiana 47907

S. Glenn, Y. Kwon,* A. L. Lyon, and E. H. Thorndike

University of Rochester, Rochester, New York 14627

C. P. Jessop, K. Lingel, H. Marsiske, M. L. Perl, V. Savinov, D. Ugolini, and X. Zhou

Stanford Linear Accelerator Center, Stanford University, Stanford, California 94309

T. E. Coan, V. Fadeyev, I. Korolkov, Y. Maravin, I. Narsky, R. Stroynowski, J. Ye, and T. Wlodek

Southern Methodist University, Dallas, Texas 75275

M. Artuso, R. Ayad, E. Dambasuren, S. Kopp, G. Majumder, G. C. Moneti, R. Mountain, S. Schuh, T. Skwarnicki, S. Stone, A. Titov, G. Viehhauser, and J. C. Wang

Syracuse University, Syracuse, New York 13244

     61 052002-1

S. E. Csorna, K. W. McLean, S. Marka, and Z. Xu
Vanderbilt University, Nashville, Tennessee 37235

R. Godang, K. Kinoshita,[†] I. C. Lai, P. Pomianowski, and S. Schrenk
Virginia Polytechnic Institute and State University, Blacksburg, Virginia 24061

G. Bonvicini, D. Cinabro, R. Greene, L. P. Perera, and G. J. Zhou
Wayne State University, Detroit, Michigan 48202

S. Chan, G. Eigen, E. Lipeles, M. Schmidtler, A. Shapiro, W. M. Sun, J. Urheim, A. J. Weinstein, and F. Würthwein
California Institute of Technology, Pasadena, California 91125

D. E. Jaffe, G. Masek, H. P. Paar, E. M. Potter, S. Prell, and V. Sharma
University of California, San Diego, La Jolla, California 92093

D. M. Asner, A. Eppich, J. Gronberg, T. S. Hill, D. J. Lange, R. J. Morrison, H. N. Nelson, T. K. Nelson,
J. D. Richman, and D. Roberts
University of California, Santa Barbara, California 93106

B. H. Behrens, W. T. Ford, A. Gritsan, H. Krieg, J. Roy, and J. G. Smith
University of Colorado, Boulder, Colorado 80309-0390

J. P. Alexander, R. Baker, C. Bebek, B. E. Berger, K. Berkelman, V. Boisvert, D. G. Cassel, D. S. Crowcroft, M. Dickson,
S. von Dombrowski, P. S. Drell, K. M. Ecklund, R. Ehrlich, A. D. Foland, P. Gaidarev, R. Galik, L. Gibbons,
B. Gittelman, S. W. Gray, D. L. Hartill, B. K. Heltsley, P. I. Hopman, D. L. Kreinick, T. Lee, Y. Liu, T. O. Meyer,
N. B. Mistry, C. R. Ng, E. Nordberg, M. Ogg,[‡] J. R. Patterson, D. Peterson, D. Riley, J. G. Thayer, P. G. Thies,
B. Valant-Spaight, A. Warburton, and C. Ward
Cornell University, Ithaca, New York 14853

(CLEO Collaboration)

From a data sample of 29058 $\tau^\pm \to \pi^\pm \pi^+ \pi^- \pi^0 \nu_\tau$ decays observed in the CLEO detector we derive a 95% confidence upper limit on the tau neutrino mass of 28 MeV.

PACS number(s): 14.60.Pq, 12.15.Ff, 13.35.Dx, 23.40.Bw

I. MOTIVATION

In the standard model the tau lepton and the tau neutrino form the third generation weak doublet of leptons. Most observations are consistent with zero mass for each of the three types of neutrino, and with the conservation of lepton number for each of e, μ, τ separately. These suppositions, however, should be tested, especially in the light of recent indications [1,2] of oscillations among the neutrino species.

There are model dependent limits on the possible values of the tau neutrino mass. The SuperKamiokande experiment [2] measures the ratio of rates for ν_μ and ν_e from decay products of particles produced in cosmic ray collisions in the atmosphere. The deficit in the ν_μ rate, along with its dependence upon the neutrino zenith angle and energy, can be interpreted as due to oscillation of the ν_μ to ν_τ with a maximal amplitude ($\sin 2\theta \sim 1$) and a frequency determined by

$5 \times 10^{-4} < \Delta m^2 < 6 \times 10^{-3}$ eV^2 at 90% confidence. This would imply, if the ν_τ mass were much larger than the ν_μ mass, that

$$0.02 < m_{\nu_\tau} < 0.08 \text{ eV } (90\% \text{ C.L.}).$$

Astrophysical observations and cosmological theory limit the energy density of the universe, thus restricting the sum of *stable* neutrino masses [3]. This leads to the limit

$$m_{\nu_\tau} < 24 \text{ eV}.$$

This limit not only depends on ν_τ being stable, but also varies with the value of the Hubble constant and other inputs.

The possible effects of the tau neutrino on big-bang nucleosynthesis lead to either a low mass ν_τ or to a decaying ν_τ at higher mass [4]:

$$m_{\nu_\tau} < 0.37 \text{ MeV} \quad \text{or} \quad m_{\nu_\tau} > 18 \text{ MeV}.$$

The width of the excluded region increases with the lifetime of the ν_τ and also depends on the assumed abundance of light elements.

The standard model relations among the τ and μ masses and lifetimes and some τ branching fractions [5] imply

---

TABLE I. 95% confidence upper limits on m_{ν_τ} obtained from kinematics of τ decays.

Experiment	Ref.	Decay	MeV
ALEPH	[15]	$3\pi^\pm$	25.7
		$5\pi^\pm(\pi^0)$	23.1
OPAL	[16]	$5\pi^\pm$	43.2
		$3\pi^\pm$	35.3
ARGUS	[17]	$5\pi^\pm$	31
CLEO	[14]	$5\pi^\pm, 3\pi^\pm 2\pi^0$	30
	This analysis	$3\pi^\pm \pi^0$	28

$$m_{\nu_\tau} < 48 \text{ MeV}.$$

The popular seesaw mechanism for generating neutrino masses [6] postulates the relation

$$m_{\nu_e} : m_{\nu_\mu} : m_{\nu_\tau} = m_e^2 : m_\mu^2 : m_\tau^2.$$

This would imply rather weak limits on the ν_τ mass:

$$m_{\nu_\tau} < 180 \text{ MeV}, \quad \text{from } m_{\nu_e} < 15 \text{ eV},$$

$$m_{\nu_\tau} < 48 \text{ MeV}, \quad \text{from } m_{\nu_\mu} < 0.17 \text{ MeV}.$$

The model dependences in all of these limits on the ν_τ mass argue for a more direct measurement. The observation of the decay of accelerator produced taus along with measurements of the energy and momentum of the detectable daughter products (all but the ν_τ) can constrain the possible values for m_{ν_τ}, especially in cases when the effective mass of the detected particles is close to m_τ. Because the cross section for $\tau^+ \tau^-$ production is up to 15% of the total $e^+ e^-$ annihilation cross section, an electron-positron collider is a natural choice for the source of taus.

One looks for a hadronic decay mode with only one neutrino in the final state. Most of the previous measurements (see Table I) have been made with the higher multiplicity decay modes in which the effective mass of the hadrons is more likely to be close to the kinematic limit m_τ with the maximum sensitivity to m_{ν_τ}. All such decay modes are strongly phase-space suppressed, however, and the branching fractions are very low. An alternative strategy, which we use in the present measurement, is to pick a decay mode with a lower hadron multiplicity but with a much larger branching fraction. Although the four-pion decay, $\tau^- \to \pi^- \pi^+ \pi^- \pi^0 \nu_\tau$, relative to the five-pion decay, produces a smaller proportion of events in which the effective hadronic mass is close to m_τ, the branching fraction is 4.2%, as compared to $\sim$0.1% for the higher multiplicity modes.

II. DATA SAMPLE AND EVENT SELECTION

The experiment was performed using the Cornell Electron-positron Storage Ring and the CLEO II detector, described elsewhere [7]. Charged particle tracks were recon-

structed in three nested cylindrical drift chambers in a solenoid field of 1.5 T. The mean-squared resolution in momentum transverse to the beam was $(\delta p_T / p_T)^2 = 0.005^2 + (0.0015 \text{ GeV}^{-1} \times p_T)^2$. Photon and electron showers were detected over 98% of 4π steradians in an array of 7800 CsI scintillation counters with an energy resolution of $\delta E/E = 0.0035/E^{0.75} + 0.019 - 0.001E$ (E in GeV) in the central region of the polar angle, $45° < \theta < 135°$. Ionization, time of flight, and shower energy aided in lepton identification.

The data used in the present analysis were from 4.75 fb^{-1} of accumulated luminosity, two-thirds at 10.58 GeV and one-third at 10.52 GeV $e^+ e^-$ center of mass energies. This corresponds to 4.3×10^6 $\tau^+ \tau^-$ pairs produced.

We determined event selection criteria using Monte Carlo simulated signal and background data samples. We selected the one–versus–three-track topology with zero net charge, that is, events containing a three-charged-track tau decay candidate tagged by a single-prong decay in the opposite hemisphere. Tracks were accepted in the polar angle range $|\cos \theta| < 0.9$. The three signal tracks each had to have $p_T > 0.019 E_{beam}$ and had to fail electron identification criteria [8]. The tag track had to have momentum greater than $0.047 E_{beam}$ and had to be consistent with one of four possible decay modes

$$\tau^+ \to e^+ \nu_e \overline{\nu_\tau},$$

$$\tau^+ \to \mu^+ \nu_\mu \overline{\nu_\tau},$$

$$\tau^+ \to \pi^+ \overline{\nu_\tau},$$

$$\tau^+ \to \rho^+ \overline{\nu_\tau},$$

or the charge conjugates. This resulted in a data sample of 813000 tagged three-prong tau decay candidates.

On the three-prong side each event was required to have a π^0, defined as two CsI calorimeter showers in the polar angle range $|\cos \theta| < 0.71$, not matched to charged tracks, with lateral shower profiles consistent with photons, and with effective mass in the range $120 < m_{\gamma\gamma} < 150$ MeV. The π^0 in the decay of the ρ^+ in the $\tau^+ \to \rho^+ \overline{\nu_\tau}$ tag channel also had to satisfy these requirements, along with $E_\gamma > 50$ MeV for each photon and $m(\pi^+ \pi^0) < 1.5$ GeV. Non-photon calorimeter showers can make false π^0 candidates. These typically originate from nuclear interactions of the charged pions in the CsI crystals producing secondaries isolated from any charged track. If several π^0 candidates were found on the three-prong side of an event, we kept only the one with the highest energy. We rejected events with an extra shower of more than 300 MeV or, if photon-like in lateral shower shape, of more than 100 MeV. The π^0 selection cuts reduced the data sample to 31305 events.

In order to minimize background from the two-photon process, for example $e^+ e^- \to e^+ e^- \gamma^* \gamma^*$, $\gamma^* \gamma^* \to \pi^+ \pi^+ \pi^- \pi^- \pi^0$ with the final e^+ and e^- escaping detection at small angles to the beam, we rejected events in which the net event momentum transverse to the beam was less than 150 MeV. The final data set included 29058 events.

TABLE II. Fraction of the $\tau^- \to h^- h^+ h^- \pi^0 \nu_\tau$ data contributed by each of the signal modes, based on known branching fractions [9].

Decay mode	% of signal
$\pi^- \pi^+ \pi^- \pi^0 \nu_\tau$	92
$K_S^0 \pi^- \pi^0 \nu_\tau, \quad K_S^0 \to \pi^+ \pi^-$	3
$K^- \omega \nu_\tau, \quad \omega \to \pi^+ \pi^- \pi^0$	1.6
$K^- K^+ \pi^- \pi^0 \nu_\tau$	1.5
$K^- K_S^0 \pi^0 \nu_\tau, \quad K_S^0 \to \pi^+ \pi^-$	1.1
$K^- \pi^+ \pi^- \pi^0 \nu_\tau$	0.5
$\omega \pi^- \pi^0 \nu_\tau, \quad \omega \to \pi^+ \pi^-$	0.2

No particle identification information was used on the charged particles. That is, decay modes in which a $K^\pm$ substitutes for a $\pi^\pm$ were considered part of the $\tau^- \to h^- h^+ h^- \pi^0 \nu_\tau$ signal. These modes contributed about 5% of the signal (see Table II). The four-pion final state includes $K_S^0 \pi^- \pi^0 \nu_\tau$, $K_S^0 \to \pi^+ \pi^-$, at 3% of the total.

The bulk of the signal is $\tau^- \to \pi^- \pi^+ \pi^- \pi^0 \nu_\tau$ (and charge conjugate). In about 53% of the events there is a $\pi^+ \pi^- \pi^0$ combination (Fig. 1) with a mass consistent with the ω (there are two possibilities per event). The two-pion mass spectra (Fig. 2) for events with no ω show ρ peaks in $\pi^+ \pi^0$ (21% per event), $\pi^- \pi^0$ (17% per event), and $\pi^+ \pi^-$ ($<2\%$ per event). The overall four-pion mass spectrum (Fig. 3) has a broad maximum around 1.2–1.4 GeV for the $\omega \pi^-$ events and a peak at 1.4 GeV for the rest of the events. There is no obvious resonance structure in $m_{4\pi}$, although the two four-pion spectra fit well each to a sum of $\rho(770)$, $\rho(1450)$, and $\rho(1700)$ with adjustable relative amplitudes and phases.

III. ANALYSIS

Conservation of energy and momentum imply that

$$m_{\nu_\tau}^2 = (E_{beam} - E_H)^2 - (\vec{p}_\tau - \vec{p}_H)^2$$

$$= m_\tau^2 + m_H^2 - 2 E_{beam} E_H$$

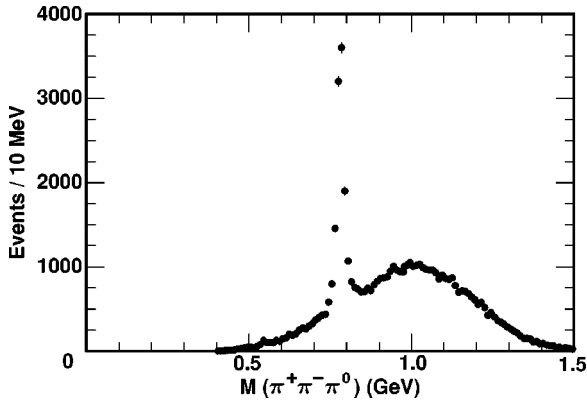$$+ 2 \sqrt{E_{beam}^2 - m_\tau^2} \sqrt{E_H^2 - m_H^2} \cos \theta_{H\tau}.$$

FIG. 1. Invariant mass distribution for $\pi^+ \pi^- \pi^0$ combinations in the data, with two entries per event. No backgrounds have been subtracted.
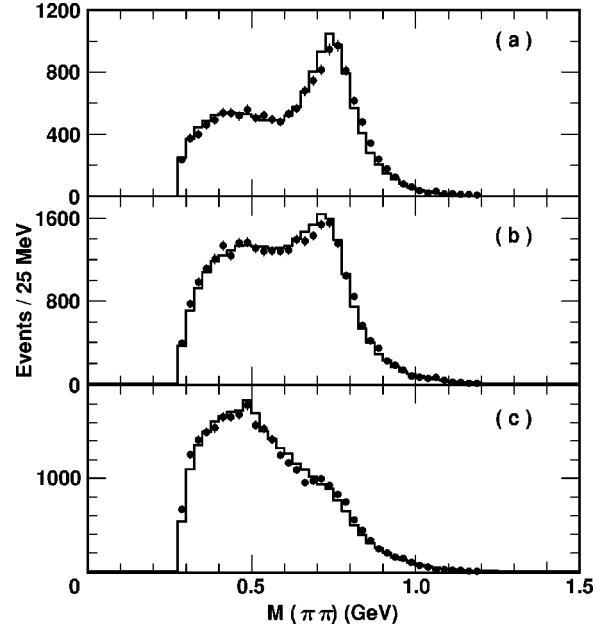

FIG. 2. Invariant mass of $\pi\pi$ combinations in events outside the ω peak: $\pi^+ \pi^0$ [(a) one entry per event], $\pi^- \pi^0$ [(b) two entries per event], $\pi^+ \pi^-$ [(c) two entries per event]. The data distribution is represented by the points with error bars and Monte Carlo calculation by the histogram.

The beam energy E_{beam} and the energy E_H and effective mass m_H of the hadronic (four-pion) system are measured in each event, and $m_\tau = 1777.05^{+0.29}_{-0.26}$ MeV is known [9,10]. Thus, if we fix m_{ν_τ}, for each allowed value of the scaled hadronic mass $x = m_H / m_\tau$ there is a range of kinematically allowed values of the scaled hadronic energy $y = E_H / E_{beam}$, where the limits are obtained by taking the last term to be at its $\cos \theta_{H\tau} = \pm 1$ limits. Figure 4 shows the distribution of the data in x, y and the boundary curves for two values of m_{ν_τ}. Even though there is background outside the kinematically allowed region, it is clear that the two-dimensional distribution of the data is sensitive to the value of m_{ν_τ}. More precisely, the likelihood of the observed x, y
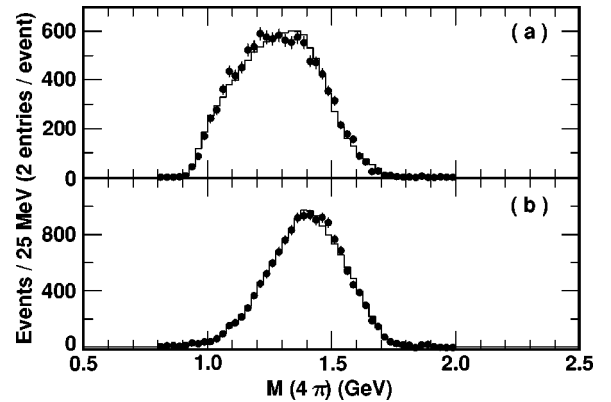

FIG. 3. Four-pion invariant mass for events within the ω peak (a) and outside the ω peak (b). The data distribution is represented by the points with error bars and Monte Carlo calculations by the histogram.
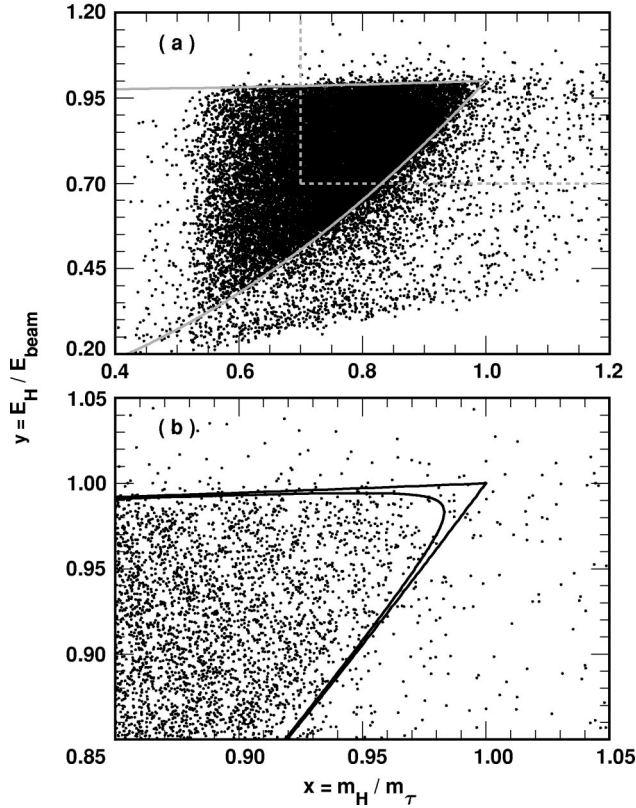
FIG. 4. Distribution in scaled hadronic energy versus scaled hadronic mass for events in the final data sample, shown for the full range (a) and for a restricted range near the kinematic end point (b). The curves show the boundaries of the allowed kinematic region for $\tau \to \pi^- \pi^+ \pi^- \pi^0 \nu_\tau$ assuming $m_{\nu_\tau} = 0$ in (a) and (b) and $m_{\nu_\tau} = 30$ MeV in (b). The dashed lines in (a) show the boundary of the fit region.

event distribution, including background, plotted for various assumed m_{ν_τ} values, can give information on which m_{ν_τ} values are consistent with experiment.

We define the likelihood for an individual event observed at x_i, y_i as the probability density $P(x_i, y_i | m_{\nu_\tau})$ of observing such an event assuming m_{ν_τ} to be the neutrino mass. $P(x_i, y_i | m_{\nu_\tau})$ contains terms for signal and backgrounds. The likelihood for the entire data sample is then the product of the event likelihoods:

$$\mathcal{L}(m_{\nu_\tau}) = \prod_{i=1}^{N} P(x_i, y_i | m_{\nu_\tau}).$$

Signal likelihood. We first discuss the signal contribution to the single-event probability density $P(x_i, y_i | m_{\nu_\tau})$. It can be expressed as the product of the spectral function (decay probability density) $\mathcal{F}$ and detection efficiency ϵ at the true x, y, convolved with the experimental resolution function $\mathcal{R}_i$ derived from data for that event:

$$P_{sig}(x_i, y_i | m_{\nu_\tau}) = \int \mathcal{F}(x, y | 0) w(x, y | m_{\nu_\tau}) \epsilon(x, y)$$

$$\times \mathcal{R}_i(x_i - x, y_i - y) dx dy.$$

For convenience we have expressed $\mathcal{F}(x, y | m_{\nu_\tau})$ in terms of the spectral function for $m_{\nu_\tau} = 0$ and a weight function that takes account of the dependence of $\mathcal{F}$ on m_{ν_τ}. The weight function w is determined from the known effect of a non-zero neutrino mass on the phase space and the kinematic boundary. It is zero outside the allowed region.

The spectral function $\mathcal{F}(x, y | 0)$ is obtained by adjusting a physics motivated 14-parameter function [8] to match distributions in the simulated data and the real data over the range $x < 0.925$, where we have verified by Monte Carlo calculations that the choice of $\mathcal{F}$ does not bias the determination of m_{ν_τ}. The function so determined is then used in the entire $x < 1$ range. It includes adjustable amplitudes and phases for $\omega \pi$ and for $\rho \pi \pi$ in all charge combinations. The $\omega \pi$ and $\rho \pi \pi$ mass spectra are each a superposition of $\rho(770)$, $\rho(1450)$, and $\rho(1700)$ resonances. The masses and widths of the resonances are fixed. We adjust the parameters by comparing distributions in simulated data, including the effects of detector acceptance and resolution, and in real data with estimated tau and non-tau backgrounds subtracted. Figures 2 and 3 illustrate the goodness of the fit.

We compute the resolution function $\mathcal{R}_i$ separately for each event. The scale of the spreading in $x - x_i$ and $y - y_i$, including x, y correlation, is obtained by propagating the resolution error matrices from the individual track and shower fits. We obtain a parametrized non-Gaussian shape from Monte Carlo calculations. The width and shape lead to distributions that match data for the reconstructed mass of $\pi^0 \to \gamma\gamma$, $K_S^0 \to \pi^+ \pi^-$, and $D \to K\pi$. The projected distributions of rms resolutions in hadronic mass and energy peak at 11 and 17 MeV in the region near the kinematic end point. By using the resolution function appropriate for each event instead of an averaged one, we diminish the effect of fluctuations from poorly measured events near the kinematic boundary.

We evaluate the integral for each event by Monte Carlo calculations, using a GEANT [11] simulation of physical processes in the CLEO detector. That is, we first generate about 1×10^6 simulated signal events using the KORALB event generator [12], tagged $\tau^- \to \pi^- \pi^+ \pi^- \pi^0 \nu_\tau$, according to the distribution $\mathcal{F}(x, y | 0)$. Then for each observed real event i and for each assumed value of m_{ν_τ} we form the following sum over all the Monte Carlo events that contribute:

$$P_{sig}(x_i, y_i | m_{\nu_\tau}) = \frac{\displaystyle\sum_{j=1}^{N_{MC}} w(x_j, y_j | m_{\nu_\tau}) \mathcal{R}_i(x_i - x_j, y_i - y_j)}{\displaystyle\sum_{j=1}^{N_{MC}} w(x_j, y_j | m_{\nu_\tau})}.$$

We take account of the efficiency factor ϵ by omitting the Monte Carlo events that are not detected by the simulated CLEO detector or recognized by the event selection criteria. The Monte Carlo integration technique enables us to include in P_{sig} the effect of initial state radiation, $e^+ e^- \to \tau^+ \tau^- \gamma$. Radiative events have a lower effective E_{beam}, causing them to be produced with lower apparent y. Some of them can be seen in Fig. 4 below the lower no-radiation kinematic limit. The Monte Carlo calculation also includes the appropriate

number of events from the $K_S \to \pi^+ \pi^-$ and $K^{\pm}$-for-$\pi^{\pm}$ substitution modes (see Table II).

Background likelihood. We distinguish three types of significant background: (a) events from the two-photon process that are not eliminated by our transverse momentum cut, (b) $\tau^+ \tau^-$ events that do not contain our signal modes, and (c) non-τ hadronic events from $e^+ e^- \to q\bar{q}$ ($q = u, d, s, c$).

The two-photon events, such as $e^+ e^- \to e^+ e^- \gamma^* \gamma^*$, $\gamma^* \gamma^* \to \pi^+ \pi^+ \pi^- \pi^- \pi^0$ in which the hadronic state has enough transverse momentum to be accepted, form a background at low scaled hadron energy y that is difficult to model reliably. Since this kinematic region is insensitive to m_{ν_τ}, the best strategy is to eliminate it from the likelihood fit. The detector efficiency is also less accurately modeled at low x and low y, so we restrict the fit to $x > 0.7$, $y > 0.7$. Within this region the two-photon background can be neglected, and the detailed choice of boundary has no influence on the m_{ν_τ} limit. The cut reduces the number of data events used in the fit to 16577.

Tau decays of higher or lower multiplicity can masquerade as our signal mode if particles escape undetected and/or secondaries in the CsI crystal array are misinterpreted as photons from a π^0. We evaluate these and other misreconstruction effects by Monte Carlo simulation of the response of the CLEO detector to 12×10^6 $\tau^+ \tau^-$ events generated with the known branching fractions. Of the accepted data events in the fit region, 7.3% are from tau background. They are mainly $\tau^- \to \pi^- \pi^+ \pi^- \nu_\tau$ with a spurious π^0.

Although most hadronic $e^+ e^- \to q\bar{q}$ annihilation events are rejected by our one-versus-three-charged-track criterion, some of them can survive. The $q\bar{q}$ contamination in our data sample was evaluated by a 36×10^6 event Monte Carlo simulation using the LUND [13] generator. The simulation has been extensively tuned to produce results that agree with experiment. In particular, we have verified the agreement between data and Monte Carlo calculation for the events satisfying the one-versus-three topology but having a tag with an energy that could not come from τ decay, and for the events that have x values well above the kinematic limit for the signal τ mode. The $q\bar{q}$ background accounts for 3.1% of the accepted data events in the fit region.

The calculation of the background contribution P_{bkg} to the individual event likelihood is similar to the calculation of P_{sig}. However, since the expected background event distribution (the analogue of $\mathcal{F} \times \epsilon$) can be expressed only in terms of observed x_i, y_i, it is not appropriate to integrate over the experimental resolution function; its effect is already contained in the distribution. As the distribution is not an analytic function, but a collection of simulated events with a rather smooth distribution, we approximate the value of $P_{bkg}(x_i, y_i)$ for the i-th data event by the number (appropriately weighted) of $\tau^+ \tau^-$ and $q\bar{q}$ background Monte Carlo events per unit area in the x, y vicinity of x_i, y_i. This P_{bkg} is of course independent of m_{ν_τ}.

We sum the signal and background likelihoods for each event and take the product over all events in the region $x > 0.7$, $y > 0.7$ to form the net likelihood $\mathcal{L}$. This is repeated
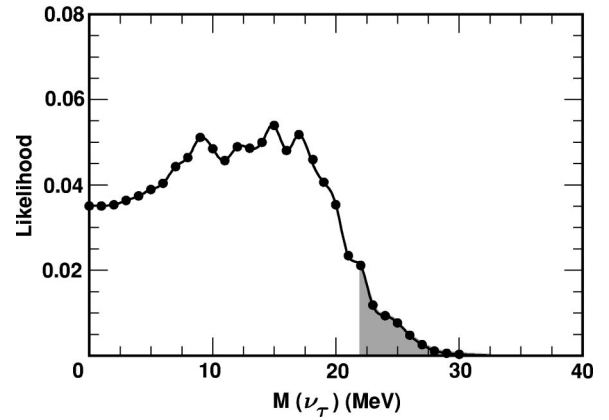

FIG. 5. The measured likelihood evaluated for a sequence of m_{ν_τ} values. The curve is a cubic spline fit through the points. The shaded area is 5% of the integral under the curve.

for a range of assumed m_{ν_τ} values to obtain $\mathcal{L}(m_{\nu_\tau})$.[1] The overall normalization of $\mathcal{L}(m_{\nu_\tau})$ is arbitrary.

IV. RESULTS

Figure 5(a) shows the likelihood as a function of assumed neutrino mass. The integral under the curve beyond 22 MeV is 5% of the total. Before interpreting this as a 95% upper limit on m_{ν_τ}, however, we have to consider systematic uncertainties that could affect the limit.[2]

The CLEO charged particle momentum measurement scale is uncertain by about 0.05%, and the π^0 energy scale is uncertain by 0.25%. This shows up as a potential mismatch between Monte Carlo simulations and data, resulting in a distortion in $\mathcal{L}(m_{\nu_\tau})$. Variations in the scale of these magnitudes cause a shift of 5.0 MeV in the 95% limit, when the two effects are combined in quadrature.

The four-pion spectral function $\mathcal{F}$ was determined by varying the contributions of the $\rho(770)$, $\rho(1450)$, and $\rho(1700)$ to match the data below $x = 0.925$, then extrapolating into the region $0.925 < x < 1$ sensitive to m_{ν_τ}.[3] The result-

---

[1] A Poisson coefficient expressing the dependence of the number of observed events on m_{ν_τ} (as used in Ref. [14]) is not used here because the large number of events in the fit region of this work is insensitive to the neutrino mass scale in question.

[2] Integrating the likelihood to extract the upper limit corresponds to a Bayesian methodology with a prior distribution uniform in m_{ν_τ} for $m_{\nu_\tau} < 30$ MeV. Integrating instead as a function of $m_{\nu_\tau}^2$ results in a 1 MeV larger limit. Under the assumption that the likelihood is Gaussian in some other function of neutrino mass (which is truncated to zero for $m_{\nu_\tau} < 0$), the limit would be 1.5 MeV larger.

[3] Note that if we were to force the spectral function to agree with the data all the way to the kinematic end point ($x = 1$), we would get a (biased) 95% limit of 17 MeV for m_{ν_τ}. This is significant in that it represents the lowest limit one could *a priori* expect to obtain with the given statistical accuracy and background, assuming $m_{\nu_\tau} = 0$.

TABLE III. Systematic uncertainty sources and the shifts they induce in the m_{ν_τ} upper limit.

Source	MeV
π^0 energy scale	3.7
Track momentum scale	3.3
Spectral function	4.0
$q\bar{q}$ and τ background corrections	0.8
Monte Carlo statistics	0.5
Resolution function	0.4
Quadrature sum	6.4

ing likelihood function (Fig. 5) is sensitive mainly to the parameters describing the $\rho(1700)$. If we vary the amplitude within the experimental accuracy of our matching and the $\rho(1700)$ mass and width within their experimental errors, we can raise the 95% likelihood limit by 4 MeV.

The effects of other systematic uncertainties have been similarly evaluated. The resulting shifts of the 95% limit on m_{ν_τ} are listed in Table III. Assuming that the various effects are independent, we combine the limit shifts in quadrature to get a net systematic shift of 6.4 MeV. Following the practice in reports of previous experiments on m_{ν_τ} limits, we add this shift linearly to the raw limit from Fig. 5:

$$m_{\nu_\tau} < 28 \text{ MeV} \quad (95\% \text{ confidence}).$$

An important difference between this measurement and ν_τ mass limits from previous e^+e^- experiments is the size of the event sample used. We observe 543 events in the sensitive portion of the kinematically allowed region, $x > 0.925$. This and the fact that we include background in the fit lead to a limit that has little sensitivity to chance fluctuations in the population of individual events near the end point. Although this experiment has its own statistical and systematic uncertainties that prevent a significant improvement in the limit value, the analysis is quite complementary to previous low statistics experiments and confirms their conclusions.

Both this measurement and the previous CLEO measurement [14] using $\tau \to 5\pi\nu_\tau$ show a broad likelihood maximum near the higher end of the allowed range of the tau neutrino mass. Since such a behavior is not unlikely even if $m_{\nu_\tau} = 0$ (as verified by Monte Carlo experiments), we do not regard it as significant. It does imply, however, that combining the results of the two CLEO measurements to make a joint likelihood curve does not significantly improve the mass limit.

[1] S.P. Mikheyev and A.Y. Smirnov, Yad. Fiz. **42**, 1441 (1985) [Sov. J. Nucl. Phys. **42**, 913 (1985)]; C. Athanassopoulos *et al.*, Phys. Rev. Lett. **75**, 2650 (1995); **77**, 3082 (1996).

[2] Y. Fukuda *et al.*, Phys. Rev. Lett. **81**, 1562 (1998).

[3] S.S. Gershtein and Ya.B. Zeldovich, Pis'ma Zh. Eksp. Teor. Fiz. **4**, 258 (1966) [JETP Lett. **4**, 174 (1966)]; R. Cowsik and J. McClelland, Phys. Rev. Lett. **29**, 669 (1972); A.S. Szalay and G. Marx, Astron. Astrophys. **49**, 437 (1976); P.J.E. Peebles, *Physical Cosmology* (Princeton University Press, Princeton, 1993).

[4] M. Kawasaki *et al.*, Nucl. Phys. **B419**, 105 (1994); J.B. Rehm, G.G. Raffelt, and A. Weiss, Astron. Astrophys. **327**, 443 (1997).

[5] J. Swain and L. Taylor, in Proceedings of the Fourth Workshop on Tau Lepton Physics, edited by J. Smith and W. Toki [Nucl. Phys. B (Proc. Suppl.) **55**, 121 (1997)].

[6] M. Gell-Mann, P. Ramond, and R. Slansky, in *Supergravity*, edited by D. Freedman and P. van Nieuwenhuizen (North-Holland, Amsterdam, 1979); T. Yanagida, in *Proceedings of the Workshop on Unified Theory and Baryon Number in the Universe*, edited by O. Sawada and A. Sugamoto (KEK, Tsukuba, 1979); R. Mohapatra and G. Senjanovic, Phys. Rev.

Lett. **44**, 912 (1980); Phys. Rev. D **23**, 165 (1981).

[7] CLEO Collaboration, Y. Kubota *et al.*, Nucl. Instrum. Methods Phys. Res. A **320**, 66 (1992).

[8] D.S. Crowcroft, Ph.D. thesis, Cornell University, 1998.

[9] Particle Data Group, C. Caso *et al.*, Eur. Phys. J. C **3**, 1 (1998).

[10] BES Collaboration, J.Z. Bai *et al.*, Phys. Rev. D **53**, 20 (1996).

[11] R. Brun *et al*, computer code GEANT v. 3.15, Report No. CERN DD/EE/84-1.

[12] S. Jadach and Z. Was, Computer codes KORALB (v.2.2)/ TAUOLA (v.2.4), Comput. Phys. Commun. **36**, 191 (1985); **64**, 267 (1991); S. Jadach, J.H. Kühn, and Z. Was, *ibid.* **64**, 275 (1991); **70**, 69 (1992); **76**, 361 (1993).

[13] S.Sjöstrand, LUND 7.3, Report No. CERN-TH-6488-92, 1992.

[14] CLEO Collaboration, R. Ammar *et al.*, Phys. Lett. B **431**, 209 (1998).

[15] ALEPH Collaboration, R. Barate *et al.*, Eur. Phys. J. C **2**, 395 (1998).

[16] OPAL Collaboration, K. Ackerstaff *et al.*, Eur. Phys. J. C **5**, 229 (1998).

[17] ARGUS Collaboration, H. Albrecht *et al.*, Phys. Lett. B **292**, 221 (1992).